DOI: https://doi.org/10.52756/ijerr.2024.v46.019 ***Int. J. Exp. Res. Rev.*, Vol. 46: 240-252 (2024)**

Original Article | *Peer Reviewed* | *Open Access*

International Journal of Experimental Research and Review (IJERR)

ISSN: 2455-4855 (Online)
www.iaph.in
ISSN 2455-4855

Experimental Investigation and Optimization of Forming Parameters in Single Point Incremental Forming of AZ31 Magnesium Alloy

Dharmin M. Patel[1] and Anishkumar H. Gandhi[2]*

[1]Department of Mechanical Engineering, Gujarat Technological University, Ahmedabad-382424, Gujarat, India;
[2]Partner, RM Legal, Surat-395007, Gujarat, India

E-mail/Orcid Id:

DP, dmp.fetr@gmail.com, https://orcid.org/0000-0001-9849-8799; *AG,* anishgandhi2002@yahoo.co.in, https://orcid.org/0000-0002-4037-6788

Article History:

Received: 11th Jul., 2024
Accepted: 21st Dec., 2024
Published: 30th Dec., 2024

Keywords:
Analysis of Variance (ANOVA), Magnesium alloy, Response Surface Methodology (RSM), Incremental Forming, Surface roughness, Taguchi's DOE

How to cite this Article:
Dharmin Patel and Anishkumar Gandhi (2024). Experimental Investigation and Optimization of Forming Parameters in Single Point Incremental Forming of AZ31 Magnesium Alloy. *International Journal of Experimental Research and Review*, *46*, 240-252.
DOI:
https://doi.org/10.52756/ijerr.2024.v46.019

Abstract: A novel and adaptable forming method, known as Single Point Incremental Forming (SPIF), has emerged to meet the growing needs of the manufacturing industry. This technique is precious for producing innovative products from sheet metal, offering enhanced flexibility and precision in fabrication. The input parameters during the forming process play a crucial role in determining the final product's formability in terms of maximum formable depth (MFD) and surface quality in terms of average surface roughness (Ra). The present research aims to optimise the forming parameters for formability and surface quality during SPIF of material AZ31 magnesium alloy. In the present research, AZ31 is selected as the target material due to its widely recognized excellent strength-to-weight ratio, making it ideal for lightweight applications in the automotive, aerospace, and electronics industries. The experiments are accomplished based on the use of a Taguchi's design of experiments. The tool diameter (TD), tool rotational speed (TRS), tool feed rate (TFR), and incremental step depth (ISD) were chosen as variable parameters and, keeping other parameters constant for maximum formable depth and average surface roughness as response parameters. The best parameter settings were found, and the statistically significant parameters of the responses were examined using the Analysis of Variance (ANOVA). The results revealed that the maximum formable depth (23.5 mm), representing the material's formability, increases with larger tool diameters (10 mm and 12 mm), and higher tool rotational speeds (5000 rpm and 6000 rpm) but decreases with higher tool feed rates (500 mm/min and 600 mm/min). On the other hand, surface roughness improves (decreases) with higher tool rotational speeds, while it increases with larger tool diameters, higher tool feed rates and greater incremental step depths. Furthermore, the findings of a confirmation experiment using the optimal conditions showed a good agreement with the experimental observation. Additionally, linear regression models for predicting the maximum forming depth and average surface roughness were developed by applying the response surface methodology (RSM), which also had good agreement with experiments conducted on optimal parameters.

Introduction

A material is formed by employing tension, compression, bending, shear, or a mixture of these loads to plastically deform it into the desired size as well as shape. Conventional forming techniques for sheet steel demand specifically for the component, expensive machines and their fabrication requires longer lead times. Again, incremental forming is a proven technique for developing alternatives for mass customization to the conventional process. Using layer-by-layer manufacturing techniques, Incremental Sheet Forming (ISF), a computer-integrated metal forming process, creates intricate 3D sheet metal components (Neugebauer et al., 2006). This procedure is carried out using a fixture to support the workpiece sheet material on a CNC milling machine. The formed object geometry is generated as a surface model in CAD software. Afterwards, Computer Aided Manufacturing (CAM) is utilized to construct the

***Corresponding Author:** anishgandhi2002@yahoo.co.in

tool pathway profile using the model. The tool path contains several contours with constant space between them. The spindle speed, expressed in revolutions per minute (RPM), is the frequency of rotation of the machine's spindle. Tool feed rate is the distance which the tool travels during one spindle revolution, measured in millimetres per revolution. The machine spindle's hemispherical-ended forming tool distorts the sheet progressively into the predetermined shape of the formed part as it advances along with created trajectories of the tool path (Li et al., 2006).

The ISF's new forming method has gained popularity during the past ten years. ISF is an emerging, established technology. During that, a sheet of metal is subjected to local plastic deformation along a predetermined path using a basic instrument (a hemispherical tip rod) (milling machine). When compared to conventional forming techniques, the fully die-free ISF process exhibits the capacity to make intricate sheet metal structures and offers better formability. It is regarded as a flexible, affordable method appropriate for making sheet metal parts in small batches and for quick prototyping (Husmann and Magnus, 2016).

This method is widely utilized in many applications like the medical, automobile, aviation and civic industries (Mcanulty et al., 2017; Yang et al., 2018; Jeswiet et al., 2005; Bao et al., 2015; Bhasker and Kumar, 2023) because of the benefits outlined above. The formability (Murugesan et al., 2021) concerns reaching the forming depth and wall angle, regulating wall thinning, minimizing the force of the forming (Min et al., 2018; Bansal et al., 2017; Nguyen et al., 2010), as well as the pillow effect, are drawbacks of this procedure, despite its obvious benefits. However, there is still a sizable demand in this process to produce parts that have a great surface quality. To determine the factors that work in generating higher surface quality, numerous scholars have done extensive research (Chang et al., 2019; Saidi et al., 2015; Villeta et al., 2011; Ji and Park, 2008; Nguyen et al., 2014).

The tool tip radius, the thickness of the sheet blank material, step size, feed, spindle speed, lubrication rate and toolpath are the primary process variables that affect forming (Galdos et al., 2012; Otsu, 2016; Duflou et al., 2008; Mulay et al., 2017; Li et al., 2015; Sharma et al., 2024). For instance, by maximizing the input factors on the roughness, the technique for employing the Taguchi method to attain better surface quality has been examined (Dureja et al., 2014). They concluded that the viscosity level, tool form and forming tool tip radius had the most influence on the frustum of the cone. Selection of the right lubricant for a tool-sheet contact can improve the surface quality of the formed components. Additionally, they discussed how speed and tool feed affected the reaction, but blank thickness, incremental depth and tool tip radius had a more subtle effect. Varying the friction force from smaller to greater at specific margins has both good and negative effects on the material's formability. Significance of lubricant selection in warm forming settings, they also asserted that solid lubrication works well to produce good surface roughness (Sivarao et al., 2014; Kumar et al., 2018; Kumar and Gulati, 2019; Bohlen et al., 2018).

Using the diameter of the tool, step size and sheet thickness as variable parameters, parametric effects have been studied on the machinability of AA2024-O sheets (Gulati et al., 2016). The results showed successful component production without breakage was achieved by combining a higher rotation speed with a thicker sheet. The impact of the mechanical properties on formability is to be assessed while incremental forming with single point tool taken tool material as DDQ Steel, HS Steel, and AA6114T4, incremental step depth, tool shape, and spindle speed as control factors are employed (Kim and Park, 2002). The best material formability in SPIF and the hardness coefficients for strain and elongation in percentage were discovered.

Considering factors like feed rate, wall angle, speed and tool diameter, breakdown detection has been examined in ISF production on aluminum alloy AA6061-T6 using the Lemaitre damage model (Chen et al., 2018). The findings show that fracture occurs during the forming process at a depth that is similar to a tool tip diameter of 8 mm and 10 mm, for an average error of 5 percent between results obtained from simulation and results found from the experiment. The variables speed, diameter of tool, z direction depth, tool feed, surface quality, and form factors of sheet material plastically formed with the ISF technique are optimized (Xu et al., 2014). Results show that feed rate and spindle speed mostly unaffected surface quality and thickness reduction. Instead, thickness reduction is dependent on any one value of wall angle, with almost 99 percent of dependence.

DOI: https://doi.org/10.52756/ijerr.2024.v46.019

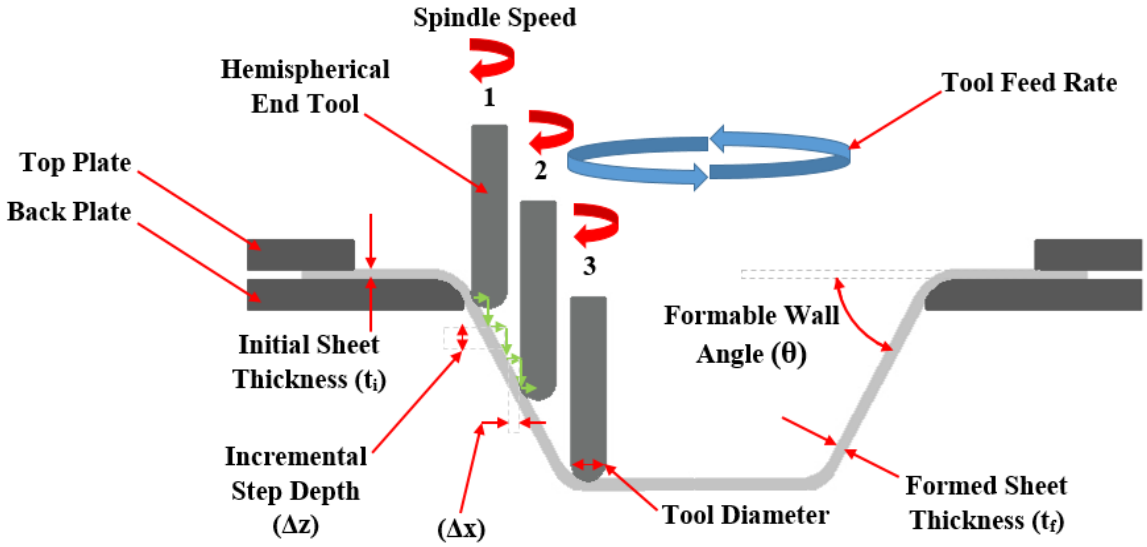

Figure 1. SPIF process parameter diagram.

AZ31 TiAl2Mn1.5 material is used for their experimental analysis using electric hot incremental forming by adopting cone and pyramid as the part geometry to consider the process parameters (Xu et al., 2016). An experimental analysis is performed for AZ31. The directional temperature effect of the magnesium alloy AZ31 using the hemispherical tool head of HSS material is examined (Dziubinska et al., 2015). An experiment is performed using Incremental forming. Laser irradiation is employed for AZ31 for local heating. A hemispherical tool head to attain cone geometry is utilized considering machining parameters such as incremental step depth, tool feed, the diameter of the tool, as well as cutting fluid (Zhang et al., 2010). ISF experiment performs for AZ31 hot air heating with carbide hemispherical tool head considering path strategy, Incremental step depth, tool feed rate, formable angle, and molybdenum disulfide (MoS_2) as a material (Ji & Park, 2008). AZ31B Mg alloy material is used for their experimental analysis using an oil bath heating-assisted WISF approach by adopting a cone as the part geometry to consider the process parameters like temperature, step depth, tool diameter and sheet thickness (Zhang et al., 2020). An experimental analysis is performed for SS 304 DDQ steel. The forming time, formed part thickness and surface quality of the SS 304 DDQ steel using the HSS tool are examined. Parameters like step depth, feed rate and spindle speed are considered (Gundarneeya et al., 2022). Ti6Al4V sheet is used for their experimental analysis using friction stir heat assisted SPIF process by adopting frustum of the cone as the part geometry (Golakiya et al., 2022).

In the present research work, the effect of four forming parameters, including tool diameter (TD), tool rotational speed (TRS), tool feed rate (TFR) and incremental step depth (ISD) for examined maximum forming depth and improved surface quality with minimum Ra of the formed components of AZ31 Magnesium alloy sheets. The experimental design was initially developed using the Taguchi L16 orthogonal array, incorporating the input parameters and their respective level configurations. After that, the forming depth and surface roughness were measured in the formed parts by the coordinate measuring machine (CMM) and surface roughness tester, respectively.

This research investigates the influence of four key forming parameters—TD, TRS, TFR and ISD—on achieving maximum forming depth and improved surface quality by minimizing surface roughness in AZ31 magnesium alloy sheets. The study utilized a Taguchi L16 orthogonal design to model the experimental setup, incorporating the input parameters and their corresponding levels. The formed parts' forming depth and surface roughness were measured using a coordinate measuring machine (CMM) and a surface roughness tester. Statistical ANOVA was performed to identify the most significant parameters influencing the responses and their optimal levels for maximizing formable depth and minimizing surface roughness. Additionally, predictive models for maximum formable depth and average surface roughness were developed using RSM, based on Taguchi design table. These models were validated through both numerical and graphical verification.

The parameters responsible for the incremental forming of the sheet, including component size after forming, depth of step, angle of wall inclination, and sheet thicknesses after and before forming, are mentioned in Figure 1. Considering every complete cycle at a

DOI: https://doi.org/10.52756/ijerr.2024.v46.019

specific height level, the '1', '2', and '3' are the incremental depth positions of the tool in sequence. A targeted model of a frustum having a pyramidal shape is generated in state-of-the-art CAD software as illustrated in Figure 2.

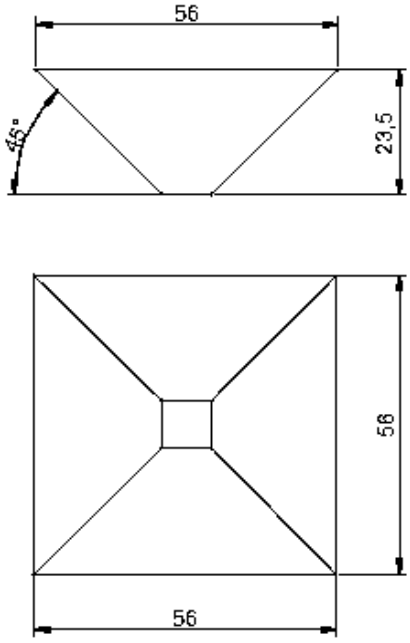

Figure 2. CAD model of a frustum of pyramidal shape.

Materials and Methods

In the present research work, magnesium alloy AZ31 has been utilized as a component material. Because of its high strength-to-weight ratio, good ductility, and less density, this material is widely utilized in the automobile industry, aerospace, electronics, textile, medical, and sports industries. The sheet of 100 mm × 100 mm × 1.1 mm size has been utilized to achieve the frustum shape of a pyramid shape for the various forming conditions. The blank material's chemical composition is stated in Table 1. A sheet of AZ31 is clamped and held by a fixture before the stated process. A pyramid-shaped frustum component with a wall angle of 45°, the largest square size of the pyramid was 56 mm × 56 mm, formed out of a sheet having 1.1 mm thickness of AZ31 by operating hemispherical end high-speed steel (HSS) tool.

Table 1. Chemical composition of Magnesium alloy (AZ31).

	Si	Ni	Cu	Fe	Ti	Ca	Mn	Zn	Al	Mg
Weight in percentage (%)	0.008	0.002	0.001	0.003	0.013	0.021	0.325	0.83	2.65	96.11

Experiments were performed using a CNC milling machine on AZ31 sheets. The maximum table motion for the CNC milling machine was 820 mm x 510 mm x 510 mm in the direction toward length, in the cross directions, and towards the headstock respectively. To hold pieces on the CNC milling machine table for sheet forming, a suitable fixture was created. The fixture is made up of three main components, the base plate, back plate, and top plate, each of which has eight circular holes with a 6 mm diameter and the ability to hold a sheet of 100 mm x 100 mm. With the help of L - key bolts, the fixture maintains the sheet borders with assurance. The support fixture is shown in Figure 3. In this shaping process, the workpiece is clamped using a fixture. As shown in Figure 5, the built-in SPIF fixture is mounted onto a CNC milling machine in the current experiment. Macro programming is used in this present study to create a spiral tool path to form a sheet material based on CAD models for the final part. Figure 5 shows a schematic of the experimental setup for the SPIF method, while Figure 4 depicts the formed frustum of pyramid-shaped components of AZ31 sheets.

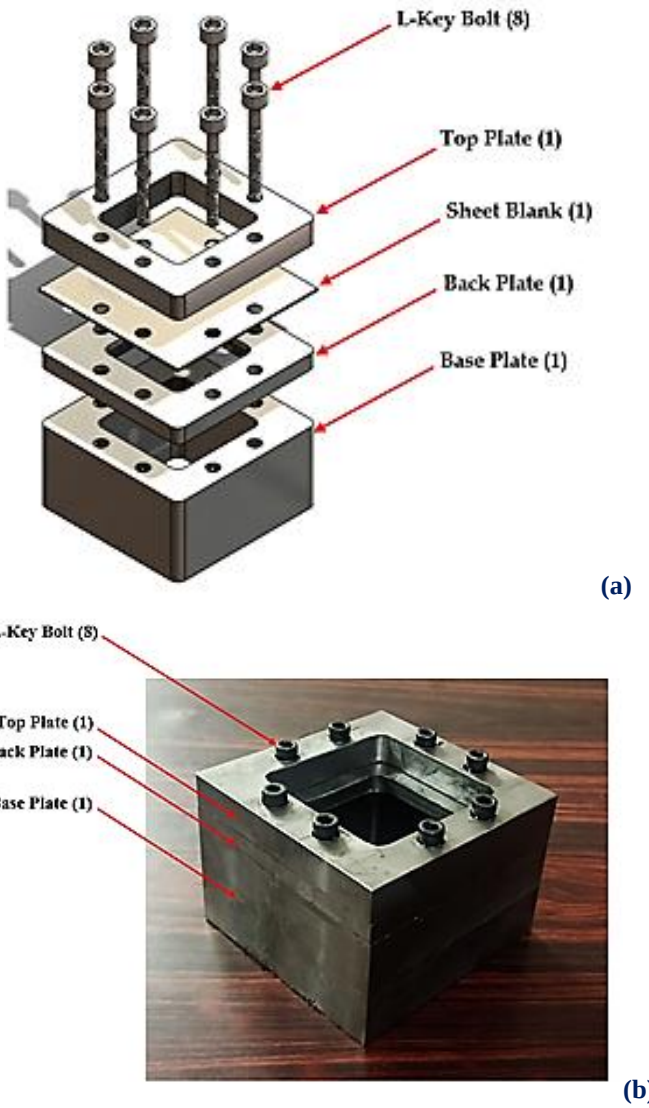

Figure 3. (a) CAD model of support fixture; (b) Actual support fixture.

DOI: https://doi.org/10.52756/ijerr.2024.v46.019

(a)

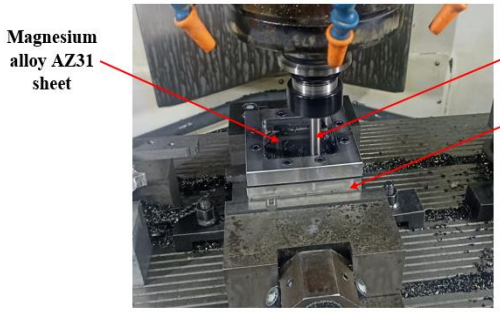

(b)

Figure 5. (a). Experimental setup for the SPIF process (b) Magnified view of the SPIF Process..

forming parameters such as TD, TRS, TFR and ISD. This study aims to identify forming parameters that influence the formability and surface quality of AZ31 as sheet material. The four-level experimental setup for TD, TRS, TFR and ISD has been attempted. From the discussion above, the L16 array has been chosen to regulate the number of experiments. Information on the chosen forming parameters and their level settings can be shown in Table 2.

Table 2. Input forming parameters with their configuration levels.

Sr. No.	Parameters	Levels			
		1	2	3	4
1	Tool Diameter - TD (mm)	6	8	10	12
2	Tool Rotational Speed – TRS (rpm)	3000	4000	5000	6000
2	Tool Feed Rate – TFR (mm/min)	300	400	500	600
3	Incremental Step Depth – ISD (mm)	0.3	0.4	0.5	0.6

The Coordinate Measuring Machine (CMM), "Mitutoyo" CRYSTA-Apex S 9108, is used to assess the

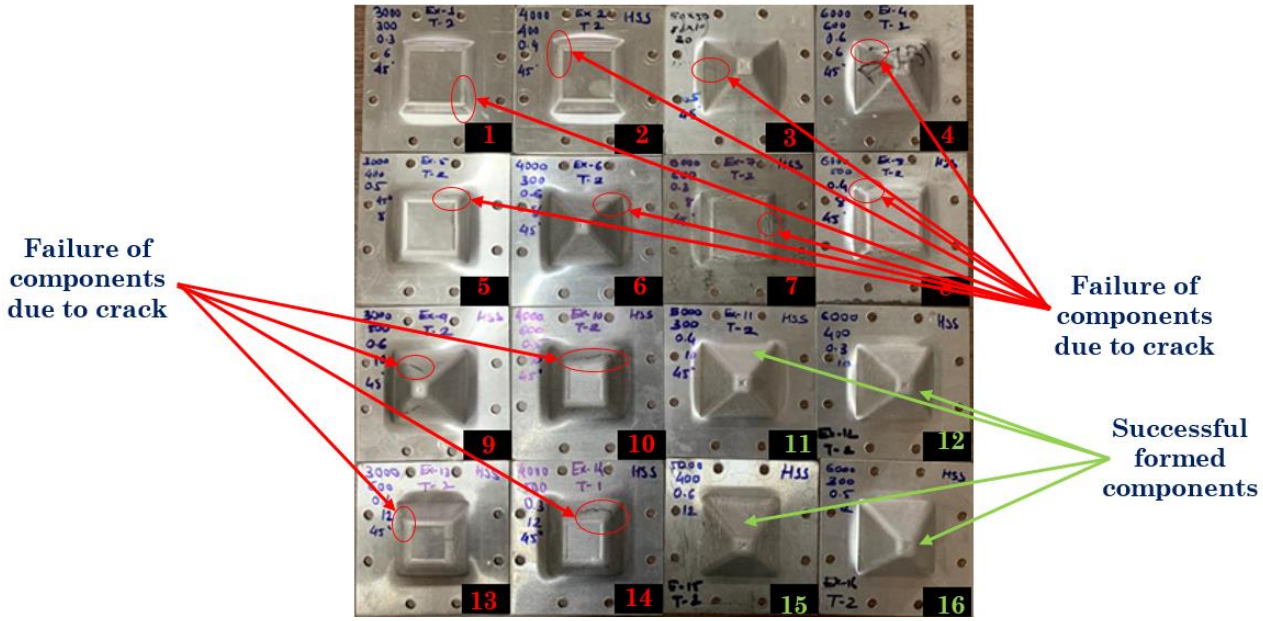

Figure 4. Formed frustum of pyramid-shaped components of AZ31 sheets.

The Taguchi method is the most appreciated approach for determining the combination of inputs and the determined outputs. The various levels of the parameters in the formation of an orthogonal array are used to find the result of the input on the outcomes. This study investigates the impact of the formability and surface quality of incrementally formed components using distribution of wall thickness and get a component profile to estimate the forming depth. The CMM is having measuring range: X axis - 900 mm, Y axis – 1000 mm, Z axis – 600 mm and resolution of 0.0001 mm. 'Mitutoyo' CRYSTA-Apex S 9108 is displayed in Figure 6(a). Profile measurement on CMM is shown in Figure 6(b).

DOI: https://doi.org/10.52756/ijerr.2024.v46.019

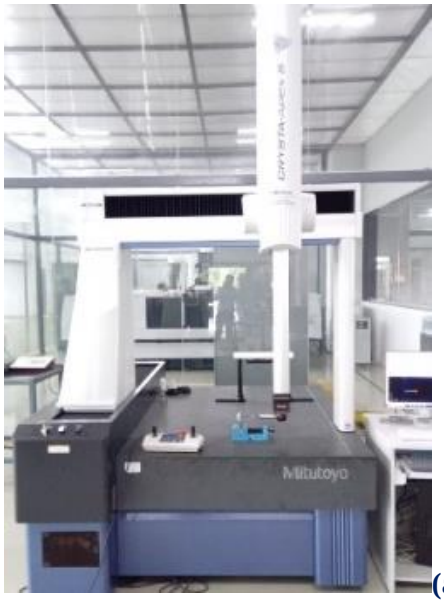

(a)

(b)

Figure 6. (a). 'Mitutoyo' CRYSTA-Apex S 9108; (b) Measurement of formed component profile.

and Gandhi, 2022). Figure 7 illustrates the measured surface roughness profiles. The Ra value of each specimen for all four walls was measured as an average value and represented to increase the statistical accuracy of results, which is summarized in Table 3.

(a)

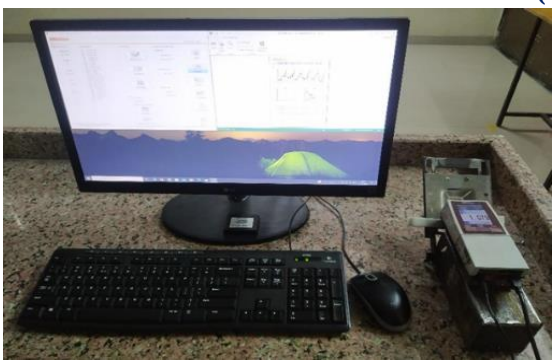

(b)

Figure 8. (a). Mitutoyo SURFTEST SJ-210; (b) Surface testing on SURFTEST SJ-210.

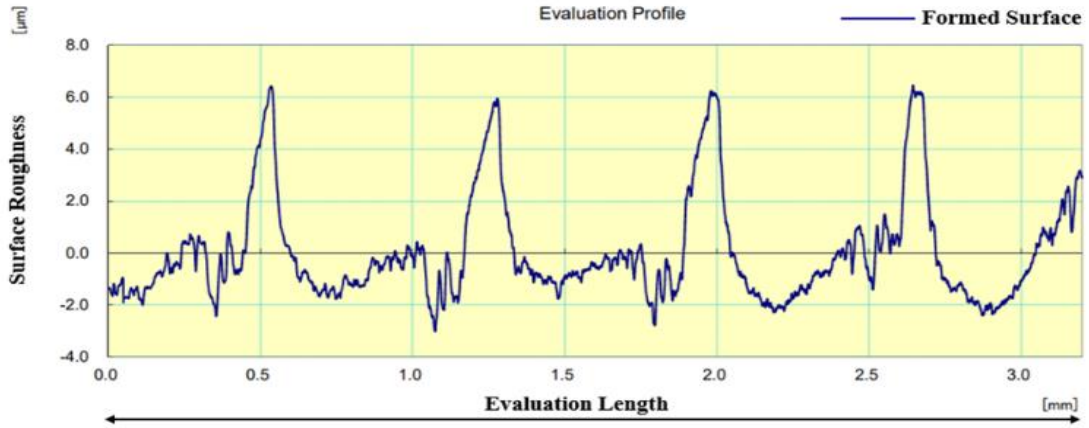

Figure 7. Surface profiles were measured for formed surfaces using the Mitutoyo SURFTEST SJ-210.

The surface roughness tester (i.e., 'Mitutoyo' SURFTEST SJ-210) is utilized to get the machined surface's average surface roughness (Ra). Mitutoyo SURFTEST SJ-210 has a capacity of 360 µm, a resolution of 0.02 µm, and a speed of 0.5 mm/s while measuring surface roughness. Mitutoyo SURFTEST SJ-210 tester is displayed in Figure 8(a). Surface testing on Mitutoyo SURFTEST SJ-210 is shown in Figure 8(b). A machined part textured is evaluated by average surface roughness (i.e., finishing of the formed surface) (Patel

For the optimization, Table 3 details are mentioned to specify the parameters that influence the responses for the formability and surface quality of the formed components. The S/N ratio has been determined on the basis of the larger-the-better for maximum formable depth and smaller-the-better for average surface roughness criterion as tabulated in Table 3. ANOVA attempts to identify the significant parameters that influence the responses (Rizvi et al., 2024). The p-value level was set at 0.05 to assess whether the forming

DOI: https://doi.org/10.52756/ijerr.2024.v46.019

parameters significantly influenced the responses. The parameter controls the outcome significantly when the p-value is not greater than 0.05. ANOVA is employed using the Minitab-21 application as a statistical tool to calculate the S/N ratio and means of the parameters and their associated outcome responses. With single response optimization, plots for the parameters have been generated based upon the mean of the S/N ratio.

Table 3. Experimental plan, results, and their evaluated S/N ratios.

Runs	TD (mm)	TRS (rpm)	TFR (mm/ min)	ISD (mm)	Formable Depth (mm)	S/N ratio for Formable Depth	Average Surface Roughness (µm)	S/N ratio for Surface Roughness
1	6	3000	300	0.3	9.5	19.5545	1.0033	-0.0286
2	6	4000	400	0.4	10.8	20.6685	1.2678	-2.0610
3	6	5000	500	0.5	20.1	26.0639	1.4583	-3.2770
4	6	6000	600	0.6	19.2	25.6660	1.5269	-3.6763
5	8	3000	400	0.5	10.5	20.4238	1.7697	-4.9580
6	8	4000	300	0.6	18.8	25.4832	1.7146	-4.6831
7	8	5000	600	0.3	10.1	20.0864	1.0743	-0.6225
8	8	6000	500	0.4	11.3	21.0616	1.2475	-1.9208
9	10	3000	500	0.6	16.0	24.0824	1.9251	-5.6889
10	10	4000	600	0.5	14.3	23.1067	1.5893	-4.0241
11	10	5000	300	0.4	23.5	27.4214	1.2897	-2.2098
12	10	6000	400	0.3	23.5	27.4214	1.0736	-0.6169
13	12	3000	600	0.4	14.2	23.0458	1.3874	-2.8440
14	12	4000	500	0.3	13.7	22.7344	1.1908	-1.5168
15	12	5000	400	0.6	23.5	27.4214	1.6794	-4.5030
16	12	6000	300	0.5	23.5	27.4214	1.5689	-3.9121

Result and Discussion

Optimization of Forming Parameters

In order to build a prediction model and determine which process factors influence the responses, maximum formable depth, and average surface roughness, Table 3 information was taken into consideration for process parameter optimisation. The formable depth must be maximised because the primary objective of this study is to attain improved formability. In order to maximise the response, the larger-the-better criteria were used to determine the S/N ratio. Additionally, the average surface roughness must be reduced in order to improve surface quality. In order to minimise the response, the S/N ratio was chosen using the smaller-the-better criteria. The means and S/N ratios for every control parameter can be assessed in order to evaluate the impact of forming parameters on the response.

Analysis of Formable Depth

Table 4 presents the produced response table for the S/N ratios of the highest formable depth. With a delta of 3.74, the tool diameter has the greatest impact on formable depth, according to the data. Tool rotational speed, incremental step depth, and tool feed rate have the next largest effects, with deltas of 3.62, 3.21 and 1.99, respectively. Level 3 for tool diameter (TD3), level 4 for tool rotational speed (TRS4), level 1 for tool feed rate (TFR1), and level 4 for incremental step depth (ISD4) were ultimately found to have the optimal level settings.

The graph of primary effects for the highest formable depth was then obtained using the S/N ratio response table, as illustrated in Figure 9. It is evident that as the TD, TRS, and ISD rise, so does the ratio. In other words, when TFR rises, the ratio falls. The formable depth was observed to increase with larger tool diameters, likely due to the more uniform distribution of stress, which reduces the risk of tearing. Similarly, an increase in tool rotational speed enhances formable depth, possibly because the elevated heat generated at the tool-sheet interface softens the material, improving its formability and enabling greater depths. A decrease in tool feed rate also positively impacts formable depth, as lower feed rates allow for more gradual and controlled deformation. Furthermore, increasing the incremental step depth contributes to greater formable depths, potentially due to the enhanced uniformity in heating and deformation, facilitating better material flow during forming.

DOI: https://doi.org/10.52756/ijerr.2024.v46.019

Table 4. Response table for S/N ratios of formable depth.

Level	TD (mm)	TRS (rpm)	TFR (mm/min)	ISD (mm)
1	22.99	21.78	**24.97**	22.45
2	21.76	23.00	23.98	23.05
3	**25.51**	25.25	23.49	24.25
4	25.16	**25.39**	22.98	**25.66**
Delta	**3.74**	**3.62**	**1.99**	**3.21**
Rank	**1**	**2**	**4**	**3**

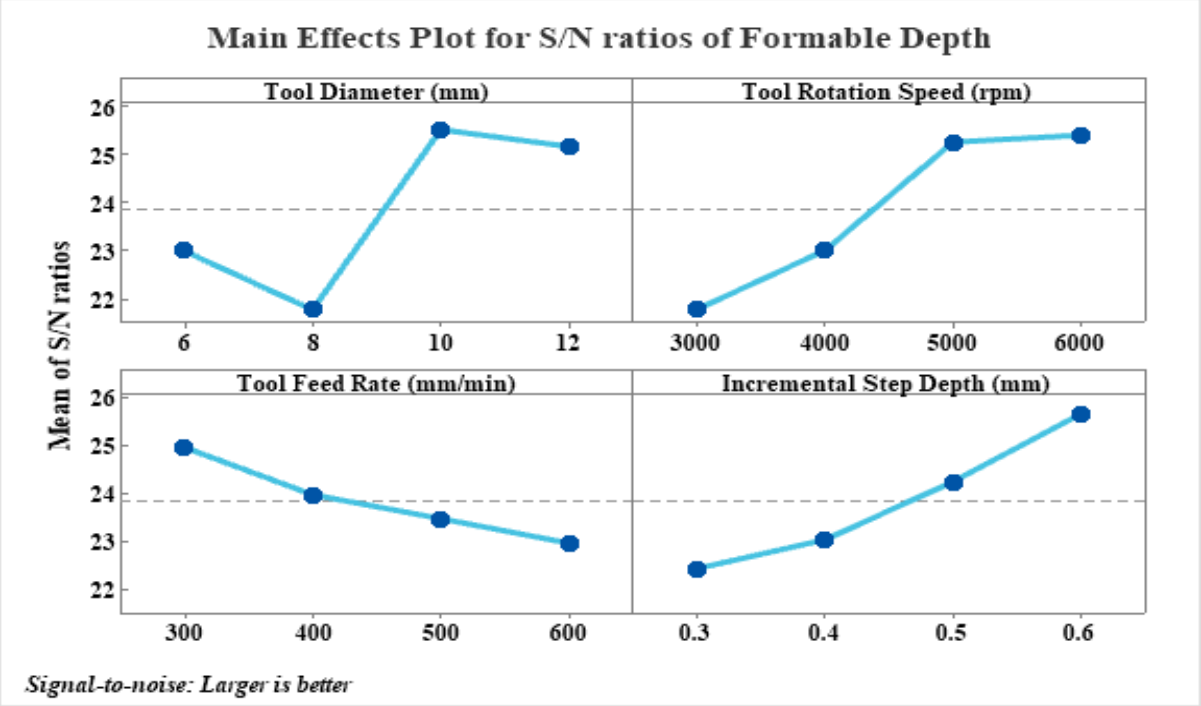

Figure 9. Main effect plot for S/N ratios of formable depth.

Analysis of Surface Roughness (Ra)

Table 5 exhibits the computed response table for the Ra S/N ratios. With a delta of 3.9416, the data show that incremental step depth has the greatest impact on Ra. Tool diameter, tool rotational speed, and tool feed rate have the next largest effects, with deltas of 0.9332, 0.8484, and 0.3925, respectively. At level 1 for tool diameter (TD1), level 4 for tool rotational speed (TRS4), level 1 for tool feed rate (TFR1), and level 1 for incremental step depth (ISD1), the ideal level setting was ultimately obtained.

Table 5. Response table for S/N ratios of Ra.

Level	TD (mm)	TRS (rpm)	TFR (mm/min)	ISD (mm)
1	**-2.2607**	-3.3799	**-2.7084**	**-0.6962**
2	-3.0461	-3.0712	-3.0347	-2.2589
3	-3.1349	-2.6531	-3.1009	-4.0428
4	-3.1940	**-2.5315**	-2.7917	-4.6378
Delta	**0.9332**	**0.8484**	**0.3925**	**3.9416**
Rank	**2**	**3**	**4**	**1**

The response table for the signal-to-noise (S/N) ratios was utilized to generate the main effects plot for surface roughness (Ra), as depicted in Figure 10. The results indicate that Ra decreases with increasing tool rotational speed (TRS) but increases with larger tool diameters (TD), higher tool feed rates (TFR), and greater incremental step depths (ISD). A smaller tool diameter was found to increase Ra, likely due to the concentrated deformation leading to a rougher surface. Conversely, an increase in tool rotational speed significantly reduced Ra, potentially due to the generation of additional heat at the tool-sheet interface, promoting smoother deformation. Lower tool feed rates also resulted in decreased Ra, possibly because they allow for more gradual deformation and improved material flow, producing smoother surfaces. Ra decreases with decreases in incremental step depth. This may be because the smaller incremental step depth of the tool makes finer, more gradual deformations, leaving smoother tool paths.

DOI: https://doi.org/10.52756/ijerr.2024.v46.019

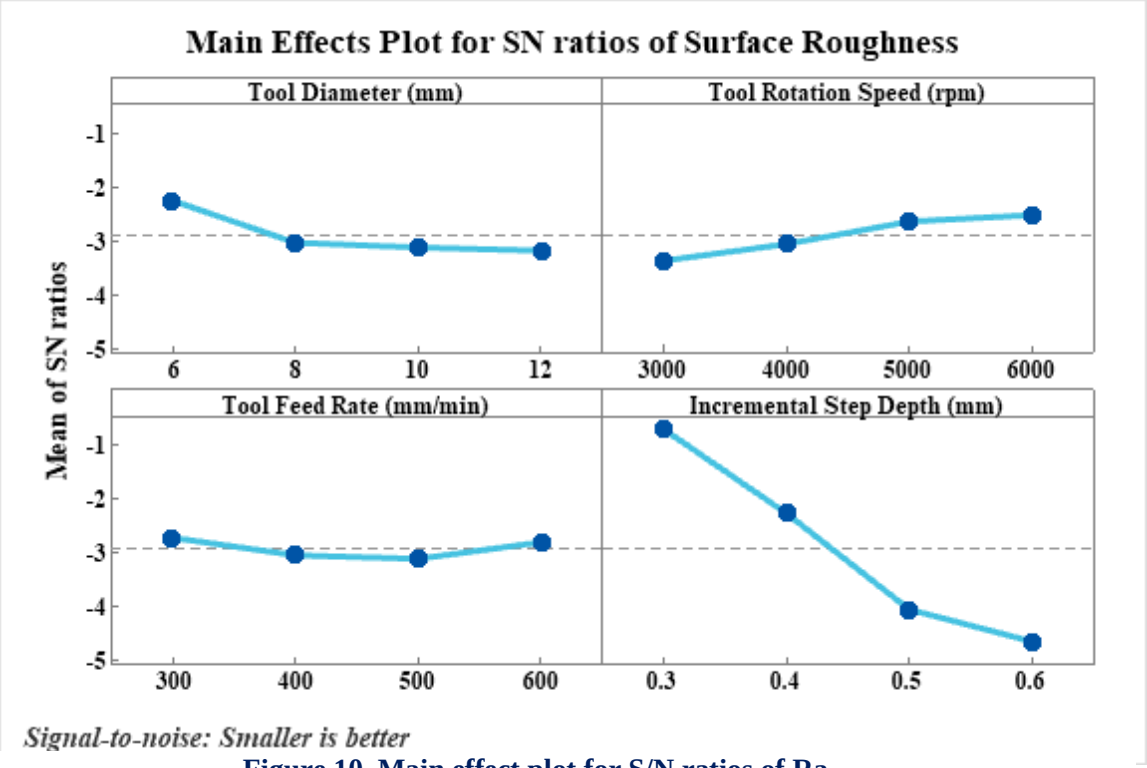

Figure 10. Main effect plot for S/N ratios of Ra

Analysis of Variance (ANOVA)

The statistical analysis of variance (ANOVA) was used to analyze the results and identify the contribution of each process parameter to the responses. The obtained ANOVA from response surface linear models are tabulated in Tables 6 and 7. It can be inferred that the tool rotational speed has the highest percentage contribution of 30.29%, followed by tool diameter of 15.46%., incremental step depth of 14.70% and tool feed rate of 10.48% on maximum formable depth. Also for Ra, the incremental step depth has the highest percentage contribution, 83.71%, followed by tool rotational speed of 5.67% and tool diameter of 3.51%.

Table 6. ANOVA for the formable depth of the formed component.

Source	Degree of freedom	Adj. SS	Adj. MS	F-Value	P-Value	Contribution
TD	1	65.70	65.70	5.85	**0.034**	**15.46 %**
TRS (rpm)	1	128.78	128.78	11.46	**0.006**	**30.29 %**
TFR (mm/min)	1	44.55	44.55	3.97	0.072	**10.48 %**
ISD (mm)	1	62.48	62.48	5.56	**0.038**	**14.70 %**
Error	11	123.60	11.24	-	-	**29.07 %**
Total	**15**	**425.11**	**312.75**	-	-	**100.00 %**

Table 7. ANOVA for the Ra of the formed component.

Source	Degree of freedom	Adj. SS	Adj. MS	F-Value	P-Value	Contribution
TD	1	0.0397	0.0397	5.43	**0.04**	**3.51%**
TRS (rpm)	1	0.0642	0.0642	8.78	**0.013**	**5.67%**
TFR (mm/min)	1	0.0000	0.0000	0.00	0.964	**0.01%**
ISD (mm)	1	0.9473	0.9473	129.61	**0.000**	**83.71 %**
Error	11	0.0804	0.0073	-	-	**7.10%**
Total	**15**	**1.1316**	**1.0585**	-	-	**100.00 %**

Confirmation Test of Taguchi-based Single Optimization

With Taguchi optimization technique, it is essential to conduct confirmation tests for optimal level of control parameters. Hence, the experiments for confirmation test are carried out at the optimum levels of process parameters with (TD3-TRS4-TFR1-ISD4) and (TD1-TRS4-TFR1-ISD1) on 1.1 mm thick AZ31 sheet for maximum formable depth and average surface roughness respectively. With Taguchi optimization technique, the

DOI: https://doi.org/10.52756/ijerr.2024.v46.019

Table 8. Confirmation Test of Taguchi-based Single optimization.

Sr. No.	Response	Optimum predicted Value	Confidence Interval Value (CI_{CE})	The Estimated optimal value with a 95% confidence interval	Result of Confirmation Test
1	Formable Depth (mm)	27.68 mm	± 6.65 mm	[21.03] < Formability Exp. < [38.92]	**23.5* mm**
2	Surface Roughness (µm)	0.8792 µm	± 0.17 µm	[0.710] < Formability Exp. < [0.887]	**0.8812 µm**
***** The maximum achievable formable depth is 23.5 mm for the designed geometry and fixture.					

95% confidence intervals CI_{CE} of expected optimal output are computed and it is presented as shown in Table 8. Predicted results were compared to the result of a confirmatory experiment. It is clear from Table 8 that the value of confirmatory results is within 95% of the confidence interval.

Modeling and its Validation

The regression model for the formable depth and surface roughness prediction was developed using the RSM while taking process parameters - TD, TRS, TFR, and ISD into account. The RSM- also known as statistical techniques for empirical modelling- is utilised to create a regression model that captures the relationship between independent and response variables. It is clear that a competent experimental design is the foundation for determining a suitable function to approximate the real connection. The experimental design derived from the Taguchi technique may be utilized to construct the prediction model since it can manage distinct variables and examine the control parameters space depending on the DOE fractional factorial arrays. Based on the results of experimentation data, Linear Regression models of formable depth and surface roughness are computed using Minitab software as mentioned below:

Forming Depth (mm) = - 4.41 + 0.906 TD + 0.002538 TRS – 0.01492 TFR + 17.68 ISD

Surface Roughness (µm) = 0.494 + 0.02228 TD – 0.000057 TRS + 0.000009 TFR + 2.176 ISD

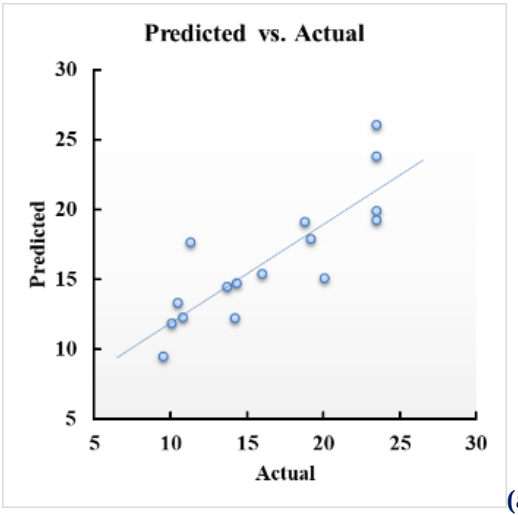

(a)

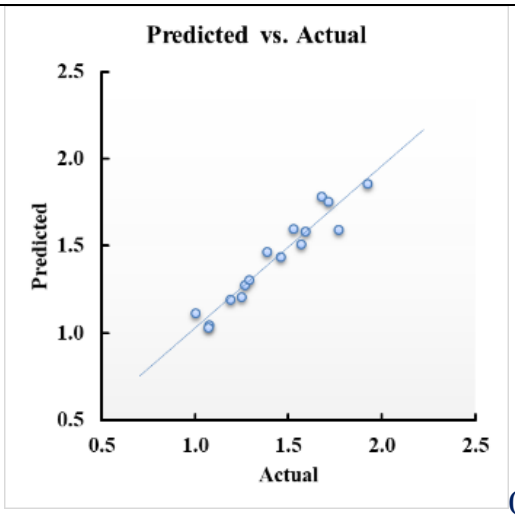

(b)

Figure 11. Plot for (a) formable depth and (b) surface roughness by experimental and predicted responses.

These formulas provide the predictable value of the formable depth and surface roughness parameter components for every combination of process parameter levels as long as the levels fall between the ranges. The values of the formable depth, surface roughness, and the limits of the factors under investigation can be predicted using the aforementioned mathematical model.

Figure 11 (a) and (b) show the graph for formable depth and surface roughness plotted against experimental and predicted values. The points are well distributed and closer to the straight line (R^2 = 60.35% for maximum formable depth and R^2 = 90.31% for average surface roughness), which gives an excellent relationship between the experimental and predicted values of maximum formable depth and average surface roughness.

Conclusion

The outcome of the current research work encompasses the forming parameter effects such as tool diameter (TD), tool rotational speed (TRS), tool feed rate (TFR), and incremental step depth (ISD) on the magnesium alloy AZ31 sheet formability in terms of maximum formable depth (MFD) and surface quality in terms of average surface roughness (Ra) for the SPIF. Taguchi and ANOVA are excellent analytical tools for finding significant machining parameters during forming to enhance the quality of the formed component. A

DOI: https://doi.org/10.52756/ijerr.2024.v46.019

surface roughness tester examines the average surface roughness of pyramid-shaped formed part walls during SPIF. A four-factor, four-level factor technique can be employed easily to develop a mathematical model for predicting maximum formable depth and average surface roughness components of forming conditions during the SPIF operation. During the present research work, the following conclusions are drawn regarding the target material, which is widely recognized for its excellent strength-to-weight ratio, making it ideal for lightweight applications in the automotive, aerospace, and electronics industries.

#The formability in terms of maximum formable depth of the formed component was found to decrease with an increase in TFR, whereas formability increases with an increase in TD, TRS, and ISD. Experimental results showed that speed TD of 10 mm, TRS of 6000 rpm, TFR of 300 mm/min and ISD of 0.6 mm resulted in the optimal parametric condition for maximum formable depth of the components produced during the SPIF process. According to ANOVA statistical analysis, all the selected parameters were found significant for the maximum formable depth of the components except TFR. TRS was the most dominating factor with a contribution of 30.29% followed by TD (i.e., 15.46%), ISD (i.e., 14.70%) and TFR (i.e., 10.48%) for formable depth.

#The surface quality in terms of surface roughness of the formed component was found to decrease with an increase in TRS, whereas surface roughness increases with an increase in TD, TFR, and ISD. Experimental results showed that speed TD of 6 mm, TRS of 6000 rpm, TFR of 300 mm/min and ISD of 0.3 mm resulted in the optimal parametric condition for better surface quality of the components produced during the SPIF process. According to ANOVA statistical analysis, all the selected parameters were found significant for the surface roughness of the components except TFR. ISD was the most dominating factor, with a contribution of 83.71 %, followed by TRS (5.67 %), TD (3.51 %) and TFR (0.01 %) for average surface roughness.

#Confirmation tests, which were conducted at optimum levels of input parameters, it shows that maximum formable depth (i.e., 23.5 mm) and surface roughness (i.e., 0.8812 µm) values were within the confidence interval at 95% confidence level and close to predicted results (i.e., 27.68 mm & 8792 µm, respectively).

#Linear regression models of formable depth and average surface roughness (Ra) were computed using Minitab® software for the prediction of formable depth and average surface roughness as a function of TD, TRS, TFR & ISD.

#The developed regression models with R^2 values of 0.6035 & 0.9031, nearer to 1 (less variance), demonstrate strong predictive accuracy for forecasting formability and surface quality, respectively. Further regression models of formable depth and average surface roughness also agree with the experiments conducted on optimal parameters.

Acknowledgement

The laboratory facilities and support for this study were provided by the R. N. G. Patel Institute of Technology – Bardoli and SETU (Science, Engineering, and Technological Upliftment) Foundation – Surat, for which the authors are sincerely grateful.

Conflict of Interest

The authors declare no conflict of interest.

References

Bansal, A., Lingam, R., Yadav, S. K., & Reddy, N. V. (2017). Prediction of forming forces in single point incremental forming. *Journal of Manufacturing Processes*, *28*(3), 486-493. https://doi.org/10.1016/j.jmapro.2017.04.016

Bao, W., Chu, X., Lin, S., & Gao, J. (2015). Experimental investigation on formability and microstructure of AZ31B alloy in electropulse-assisted incremental forming. *Materials & Design*, *87*, 632-639. https://doi.org/10.1016/j.matdes.2015.08.072

Bhasker, R. S., & Kumar, Y. (2023). Process capabilities and future scope of Incremental Sheet Forming (ISF). *Materials Today: Proceedings*, *72*(3), 1014-1019. https://doi.org/10.1016/j.matpr.2022.09.120

Bohlen, J., Cano, G., Drozdenko, D., Dobron, P., Kainer, K. U., Gall, S., Müller, S., & Letzig, D. (2018). Processing Effects on the Formability of Magnesium Alloy Sheets. *Metals*, *8*(2), 147. https://doi.org/10.3390/met8020147

Chang, Z., Li, M., & Chen, J. (2019). Analytical modeling and experimental validation of the forming force in several typical incremental sheet forming processes. *International Journal of Machine Tools and Manufacture*, *140*, 62-76. https://doi.org/10.1016/j.ijmachtools.2019.03.003

Chen, M. -S., Yuan, W. -Q., Li, H. -B., & Zou, Z. -H. (2018). New insights on the relationship between flow stress softening and dynamic recrystallization behavior of magnesium alloy AZ31B. *Materials Characterization*, *147*, 173-183. https://doi.org/10.1016/j.matchar.2018.10.031

Duflou, J.R., Verbert, J., Belkassem, B., Gu, J., Sol, H., Henrard, C., & Habraken, A.M. (2008). Process window enhancement for single point incremental forming through multi-step toolpaths. *CIRP Annals*, *57*(1), 253-256. https://doi.org/10.1016/j.cirp.2008.03.030

Dureja, J. S., Singh, R., & Bhatti, M. S. (2014). Optimizing Flank Wear and Surface Roughness during Hard Turning of AISI D3 Steel by Taguchi and RSM Methods. *Production & Manufacturing Research*, *2*(1), 767–783. https://doi.org/10.1080/21693277.2014.955216

Dziubinska, A., Gontarz, A., Horzelska, K., & Pieśko, P. (2015). The Microstructure and Mechanical Properties of AZ31 Magnesium Alloy Aircraft

Brackets Produced by a New Forging Technology. *Procedia Manufacturing*, *2*, 337-341. https://doi.org/10.1016/j.promfg.2015.07.059

Galdos, L., Sáenz de Argandoña, E., Ulacia, I., & Arruebarrena, G. (2012). Warm Incremental Forming of Magnesium Alloys Using Hot Fluid as Heating Media. *Key Engineering Materials*, pp. 504-506, 815-820. https://doi.org/10.4028/www.scientific.net/kem.504-506.815

Golakiya, V. D., & Chudasama, M. K. (2022). Experimental Formability Study of Ti6Al4V Sheet Metal using Friction Stir Heat Assisted Single Point Incremental Forming Process. *International Journal of Engineering Transactions C: Aspects*, *35*(3), 560-566. https://doi.org/10.5829/ije.2022.35.03C.08

Gulati, V., Aryal, A., Katyal, P., & Goswami, A. (2016). Process Parameters Optimization in Single Point Incremental Forming. *Journal of The Institution of Engineers (India): Series C*, *97*, 185–193. https://doi.org/10.1007/s40032-015-0203-z

Gundarneeya, T. P., Golakiya, V. D., Ambaliya, S. D. & Chauhan, K. K. (2022). Optimization of single point incremental forming process through experimental investigation on SS 304 DDQ steel. *Materials Today: Proceedings*, *57*(2), 753-760. https://doi.org/10.1016/j.matpr.2022.02.283

Husmann, T., & Magnus, C. S. (2016). Thermography in incremental forming processes at elevated temperatures. *Measurement*, *77*, 16-28. https://doi.org/10.1016/j.measurement.2015.09.004

Jeswiet, J., Micari, F., Hirt, G., Bramley, A., Duflou, J., & Allwood, J. (2005). Asymmetric Single Point Incremental Forming of Sheet Metal. *CIRP Annals*, *54*(2), 88-114. https://doi.org/10.1016/S0007-8506(07)60021-3

Ji, Y. H., & Park, J. J. (2008). Formability of magnesium AZ31 sheet in the incremental forming at warm temperature. *Journal of Materials Processing Technology*, *201*(1-3), 354-358. https://doi.org/10.1016/j.jmatprotec.2007.11.206

Kim, Y. H., & Park J. J. (2002). Effect of Process Parameters on Formability in Incremental Forming of Sheet Metal. *Journal of Materials Processing Technology*, 130-131, 42-46. https://doi.org/10.1016/S0924-0136(02)00788-4

Kumar, A., & Gulati, V. (2019). Experimental Investigation and Optimization of Surface Roughness in Negative Incremental Forming. *Measurement*, *131*, 419-430. https://doi.org/10.1016/j.measurement.2018.08.078

Kumar, A., Soota, T., & Kumar, J. (2018). Optimisation of Wire-Cut EDM Process Parameter by Grey-Based Response Surface Methodology. *Journal of Industrial Engineering International*, *14*, 821–829. https://doi.org/10.1007/s40092-018-0264-8

Li, Y., Chen, X., Liu, Z., Sun, J., Li, F., Li, J., & Zhao, G. (2006). A review on the recent development of incremental sheet-forming process. *The International Journal of Advanced Manufacturing Technology*, *92*, 2439–2462. https://doi.org/10.1007/s00170-017-0251-z

Li, Y., Lu, H., Daniel, W. J. T., & Meehan, P. A. (2015). Investigation and Optimization of Deformation Energy and Geometric Accuracy in the Incremental Sheet Forming Process using Response Surface Methodology. *The International Journal of Advanced Manufacturing Technology*, *79*, 2041-2055. https://doi.org/10.1007/s00170-015-6986-5

Mcanulty, T., Jeswiet, J., & Doolan, M. (2017). Formability in single point incremental forming: a comparative analysis of the state of the art. *CIRP Journal of Manufacturing Science and Technology*, *16*, 43-54. https://doi.org/10.1016/j.cirpj.2016.07.003

Min, J., Kuhlenkotter, B., Shu, C., Storkle, D., & Thyssen, L. (2018). Experimental and numerical investigation on incremental sheet forming with flexible die-support from metallic foam. *Journal of Manufacturing Processes*, *31*, 605-612. https://doi.org/10.1016/j.jmapro.2017.12.013

Mulay, A., Ben, S., Ismail, S., & Kocanda, A. (2017). Experimental investigations into the effects of SPIF forming conditions on surface roughness and formability by design of experiments. *Journal of the Brazilian Society of Mechanical Sciences and Engineering*, *39*, 3997-4010. https://doi.org/10.1007/s40430-016-0703-7

Murugesan, M., Bhandari, K. S., Sajjad, M., & Jung, D. (2021). Investigation of Surface Roughness in Single Point Incremental Sheet Forming Considering Process Parameters. *International Journal of Mechanical Engineering and Robotics Research*, *10*(8), 443-451. https://doi.org/10.18178/ijmerr.10.8.443-451

Neugebauer, R., Altan, T., Geiger, M., Kleiner, M., & Sterzing, A. (2006). Sheet metal forming at elevated temperatures. *CIRP Annals*, *55*(2), 793–816. https://doi.org/10.1016/j.cirp.2006.10.008

Nguyen, D. T., Park, J. G. & Kim, Y. S. (2010). Ductile Fracture Prediction in Rotational Incremental Forming for Magnesium Alloy Sheets Using Combined Kinematic/Isotropic Hardening Model. *Metallurgical and Materials Transactions A*, *41*, 1983-1994. https://doi.org/10.1007/s11661-010-0235-1

Nguyen, N. T., Seo, O. S., Lee, C. A., Lee, M. G., Kim, J. H., & Kim, H. Y. (2014). Mechanical Behavior of AZ31B Mg Alloy Sheets under Monotonic and Cyclic Loadings at Room and Moderately Elevated Temperatures. *Materials*, *7*(2), 1271-1295. https://doi.org/10.3390/ma7021271

Otsu, M. (2016). Excellent Formability of Light Metals Sheets by Friction Stir Incremental Forming. *Key Engineering Materials*, *716*, 3-10. https://doi.org/10.4028/www.scientific.net/KEM.716.3

Patel, D., & Gandhi, A. (2022). A review article on process parameters affecting Incremental Sheet Forming (ISF). *Materials Today: Proceedings*, *63*, 368-375. https://doi.org/10.1016/j.matpr.2022.03.208

Rizvi, S. A. H., Sahu, R., Siddiqui, S. A., Shah, K. K., Bajpai, V. K., & Lal, B. (2024). Assessment of Recast Layer while Machining Die Steel D3 on EDM. *International Journal of Experimental Research and Review*, *41*(Spl Vol), 96-105. https://doi.org/10.52756/ijerr.2024.v41spl.008

Saidi, B., Boulila, A., Ayadi, M., & Nasri, R. (2015). Experimental force measurements in single point incremental sheet forming SPIF. *Mechanics & Industry*, *16*(4). https://doi.org/10.1051/meca/2015018

Sharma, M., Bhattacharya, A., & Paul, S. K. (2024). Influence of single point incremental forming on the low-cycle fatigue performance of AA6061-T6. *International Journal of Fatigue*, *178*, 107994. https://doi.org/10.1016/j.ijfatigue.2023.107994

Sivarao, S., Milkey, K. R., Samsudin, A. R., Dubey, A. K., & Kidd, P. (2014). Comparison between Taguchi Method and Response Surface Methodology (RSM) in Modelling CO_2 Laser Machining. *Jordan Journal of Mechanical and Industrial Engineering*, *8*, 35-42.

Villeta, M., Rubio, E. M., Sáenz De Pipaón, J. M., & Sebastián, M. A. (2011). Surface Finish Optimization of Magnesium Pieces Obtained by Dry Turning Based on Taguchi Techniques and Statistical Tests. *Materials and Manufacturing Processes*, *26*(12), 1503-1510. https://doi.org/10.1080/10426914.2010.544822

Xu, D. K., Lu, B., Cao, T. T., Chen, J., Long, H., & Cao, J. (2014). A comparative study on process potentials for frictional stir- and electric hot-assisted incremental sheet forming. *Procedia Engineering*, *81*, 2324-2329. https://doi.org/10.1016/j.proeng.2014.10.328

Xu, D. K., Lu, B., Cao, T. T., Zhang, H., Chen, J., Long, H., & Cao, J. (2016). Enhancement of process capabilities in electrically-assisted double sided incremental forming. *Materials & Design*, *92*, 268-280. https://doi.org/10.1016/j.matdes.2015.12.009

Yang, D. Y., Bambach, M., Cao, J., Duflou, J. R., Groche, P., Kuboki, T., Sterzing, A., Tekkaya, A. E., & Lee, C. W. (2018). Flexibility in metal forming. *CIRP Annals*, *67*(2), 743-765. https://doi.org/10.1016/j.cirp.2018.05.004

Zhang, Q., Xiao, F., Guo, H., Li, C., Gao, L., Guo, X., Han, W., & Boundarev, A. B. (2010). Warm negative incremental forming of magnesium alloy AZ31 Sheet: New lubricating method. *Journal of Materials Processing Technology*, *210*(2), 323-329. https://doi.org/10.1016/j.jmatprotec.2009.09.018

Zhang, S., Tang, G. H., Wang, W. & Jiang X. (2020). Evaluation and optimization on the formability of an AZ31B Mg alloy during warm incremental sheet forming assisted with oil bath heating. *Measurement*, *157*, 107673. https://doi.org/10.1016/j.measurement.2020.107673

How to cite this Article:

Dharmin Patel and Anishkumar Gandhi (2024). Experimental Investigation and Optimization of Forming Parameters in Single Point Incremental Forming of AZ31 Magnesium Alloy. *International Journal of Experimental Research and Review*, *46*, 240-252.

DOI : https://doi.org/10.52756/ijerr.2024.v46.019